J Mater Sci: Mater Med (2007) 18:211–223
DOI 10.1007/s10856-006-0683-8

Micro-computed tomography (μ-CT) as a potential tool to assess the effect of dynamic coating routes on the formation of biomimetic apatite layers on 3D-plotted biodegradable polymeric scaffolds

A. L. Oliveira · P. B. Malafaya · S. A. Costa · R. A. Sousa · R. L. Reis

Received: 6 July 2006 / Accepted: 19 October 2006

Abstract This work studies the influence of dynamic biomimetic coating procedures on the growth of bone-like apatite layers at the surface of starch/polycaprolactone (SPCL) scaffolds produced by a 3D-plotting technology. These systems are newly proposed for bone Tissue Engineering applications. After generating stable apatite layers through a sodium silicate-based biomimetic methodology the scaffolds were immersed in Simulated Body Fluid solutions (SBF) under static, agitation and circulating flow perfusion conditions, for different time periods. Besides the typical characterization techniques, Micro-Computed Tomography analysis (μ-CT) was used to assess scaffold porosity and as a new tool for mapping apatite content. 2D histomorphometric analysis was performed and 3D virtual models were created using specific softwares for CT reconstruction. By the proposed biomimetic routes apatite layers were produced covering the interior of the scaffolds, without compromising their overall morphology and interconnectivity. Dynamic conditions allowed for the production of thicker apatite layers as consequence of higher mineralizing rates, when comparing with static conditions. μ-CT analysis clearly demonstrated that flow perfusion was the most effective condition in order to obtain well-defined apatite layers in the inner parts of the scaffolds. Together with SEM, this technique was a useful complementary tool for assessing the apatite content in a non-destructive way.

A. L. Oliveira (✉) · P. B. Malafaya · S. A. Costa · R. A. Sousa · R. L. Reis
3B's Research Group-Biomaterials, Biodegradables and Biomimetics, Univ. of Minho, Campus Gualtar, 4710 Braga, Portugal; Dept. of Polymer Engineering, Univ. of Minho, Campus Azurém, 4780-058 Guimarães, Portugal
e-mail: analeite@dep.uminho.pt

R.L. Reis
e-mail: rgreis@dep.uminho.pt

1 Introduction

Tissue Engineering (TE) has been emerging as a striking approach to the current therapies for bone regeneration/substitution. The appropriate surface chemistry for cell attachment and proliferation is a key issue that needs to be addressed while designing a scaffold for Bone TE. To combine Ca-Ps as coatings on the outermost surface of a polymeric scaffold can be a challenging, but yet attractive approach to better promote bone formation. Several methods for producing Ca-P coatings on the surface of different biomaterials have been proposed over the years, as reviewed elsewhere [1]. The biomimetic synthesis of apatite layers under presence of simulated body fluid (SBF) solutions, initially proposed by Kokubo et al. [2], has gained attention in recent years as an alternative low-temperature coating methodology. Besides its osteoconductive properties, a biomimetic apatite layer discloses a carrier potential for biologically relevant molecules such as protein growth factors, enzymes or pharmaceutical drugs used in bone related diseases, due to the physiological operating conditions of temperature and pH.

When considering porous biodegradable polymeric scaffolds there are rather few works reporting the coating of these architectures due to the complex features related with coating composition, thickness distribution or the adhesion to the substrate. Moreover, pH changes due to possible degradation of substrates' surface during the coating process have also to be taken into consideration. Nevertheless, in our research group these biomimetic coatings have been effectively produced on the surface of starch based biodegradable polymers [3, 4]. In fact, in a previous work [3] it was possible

to overcome some of these difficulties by developing a biomimetic methodology using a sodium silicate gel as nucleating agent to produce well-defined bone-like apatite coatings covering the surfaces of starch based 3D architectures. In case of bone TE applications, dynamic mineralization environments can better mimic the *in vivo* scenario, where the flow of body fluids is present, besides being suitable to promote a homogeneous formation of the Ca-P layer in the interior of the scaffold. In this work is presented a comparative study of static and dynamic biomimetic routes for growing apatite layers on the surface of biodegradable scaffolds produced by a rapid prototyping technology. These systems are newly proposed for bone Tissue Engineering applications.

To assess the apatite content in the inner parts of a scaffold is another relevant issue that needs to be taken into consideration. Tomography using X-rays is a well established technique that is gaining popularity since the interior of the specimen can be studied in great detail, without resorting to physical sectioning nor using toxic chemicals. On the other hand, it provides precise quantitative and qualitative information on the 3D morphology of the specimen [5]. After scanning, the intact samples can be subjected to other tests, therefore resolving the problem of sample scarcity. One of the main advantages of μ-CT is that it is able to evaluate the material (polymeric or ceramic) volume based on 3D spatial distribution. It can be applied to very large [6] samples such as body parts and whole organs of humans down to the nanometre scale of a single cell [7]. This means tomography can be used in a hierarchical fashion—from the human, to an organ, a tissue and down to the cell. This technique has been used to characterize the 3D trabecular bone microarchitecture and quantify bone repair responses *in vivo* [8]. For Bone TE applications, μ-CT imaging provides an efficient, non-destructive tool to quantitatively measure the amount and distribution of mineralized matrix formation throughout 3D constructs *in vitro* [9] and *in vivo* [10]. In the herein presented study is μ-CT is proposed as a new tool for mapping the distribution of biomimetic Ca-P coatings throughout the surfaces of starch/polycaprolactone (SPCL) 3D architectures.

2 Materials and methods

2.1 Preparation of the scaffolds

As a natural polymer, starch exhibits a great potential to be used in bone related applications [11–14]. In this work, the studied material is based on a blend of starch/polycaprolactone (SPCL). The blend contains around 30% of starch and 70% of poly(epsilon-caprolactone) by weight. The selected biomaterial presents a good biological behaviour and has been proposed for Bone Tissue Engineering applications [15–17].

Rapid prototyping (RP) technologies are considered as potential routes for the production of complex scaffolds for Bone TE applications, as they present superior control over design, manufacturing and reproducibility of TE scaffolds [18]. Moreover, when coupled with adequate image acquisition software, RP allows for the production of anatomically adapted 3D scaffolds based on the patient's own defect. SPCL scaffolds were produced using a 3D plotting technology (Bioplotter, EnvisionTec GmbH, Germany). In this case, consecutive alternated layers were plotted with a $0^\circ/90^\circ/\ldots/0^\circ/90^\circ$ orientation pattern to produce cubic samples with a lateral side of $L = 5$ mm. Each layer was plotted using a distance of 2 mm between layer strands and an in-plane absolute offset distance of 1 mm between consecutive equivalent layers. 3D plotting RP enables high control over scaffold morphology, namely controlled porosity and interconnectivity.

2.2 Apatite coating formation

To produce an apatite coating on the surfaces of the obtained SPCL scaffolds a biomimetic methodology was used based on a previously developed sodium silicate methodology [3]. Briefly, the samples were "impregnated" for 1 h with a sodium silicate gel from SIGMA-ALDRICH ($Na_2SiO_3 \cdot H_2O$, containing $\sim$14% NaOH and $\sim$27% SiO_2, pH $\approx$13), under mild agitation. Sodium silicate gel was herein used with concentration and SiO_2/Na_2O molar ratio as received. After this treatment the solution with the samples was diluted with 50% vol. of distilled water and stirred for 5 min. This procedure was aimed at diminishing the viscosity of the gel in order to produce a homogeneous and thin layer of vitrified sodium silicate in the surface of the materials. The scaffolds were then removed from the solution and then dried in vacuum for 3 h and moved to a controlled atmosphere ($23 \pm 1^\circ$C; 55% RH) for 24 h. A more detailed description on the coating methodology can be found elsewhere [3].

An aqueous solution was prepared comprising all major inorganic ions present in the human's blood plasma and presenting its approximate ion concentration, in order to promote *in vitro* apatite formation. The different salts were dissolved in de-ionized H_2O and the pH adjusted to neutral using tris(hydroxymethyl)aminomethane and hydrochloric acid. This simulated body fluid solution (SBF) was developed by Kokubo and co-workers [19].

The as-treated scaffolds were immersed in the SBF solution for 7 days. During this period the solution was renewed every 2 days and an apatite layer was allowed to nucleate and grow on the surface of the samples. Following this period, the samples were divided into 3 different groups and placed in contact with a renewed SBF solution under different conditions: static, agitation by shaking in a thermostatic bath (Selecta, Unitronic, Spain, 80 strokes/min) and circulating flow perfusion in a bioreactor (volume flow

Table 1 Static and dynamic conditions for coating apatite layers on the SPCL scaffolds

Periods (days)	SBF	Conditions		
7	1 X	Static		
14	1 X	Static	Agitation	Flow perfusion
21	1.5 X	Static	Agitation	Flow perfusion
Volume of SBF available per sample		50 mL	50 mL	50 mL
Solid-to-liquid ratio		1 g/400 mL/week	1 g/400 mL/week	1 g/400 mL/week
Fluid flow		None	Turbulent flow (80 strokes/min)	Laminar flow ($Q = 4$ mL/min; $t_R = 15$ s)

SBF - Simulated body fluid solution.

rate (Q) of 4 mL/min; Residence Time (t_R) of 15 s) for periods up to 14 days. In all the conditions the total volume of SBF available per sample was 50 mL and the solution was renewed every 2 days (solid-to-liquid ratio of 1 g/400 mL/week). Table 1 summarizes the different coating conditions.

For circulating flow perfusion a special bioreactor was designed according with the schematic drawing of Fig. 1.

After 7, 14 and 21 days the samples were removed from solution, washed in distilled water and dried in a controlled atmosphere (23 ± 1°C; 55% RH).

2.3 Scanning electron microscopy (SEM) and energy dispersive spectroscopy (EDS)

The morphological characterisation to the scaffolds was carried out by Scanning Electron Microscopy (SEM) analysis, in a LEICA Cambridge S360, United Kingdom. All the samples were coated with a thin film of carbon, by ion sputtering, prior to any observation. The electron beam energy was 10 KeV and 12 KeV. The scaffolds were observed in 3 different orientations: from the top, lateral side and bottom, for the different tested periods and conditions in SBF. The corresponding cross-sections were also analysed and the thickness of the apatite layers was calculated by performing measurements in six fibres *per* scaffold (3 measurements *per* fibre). Since these coatings are constituted by fused spherical apatite nuclei they present an irregular surface. Therefore, in order to ensure that the measure would be done in the same way for all the conditions the basis of these nuclei was established as the limit for the coating. In this way the measured average values are the minimum thickness values for all the samples.

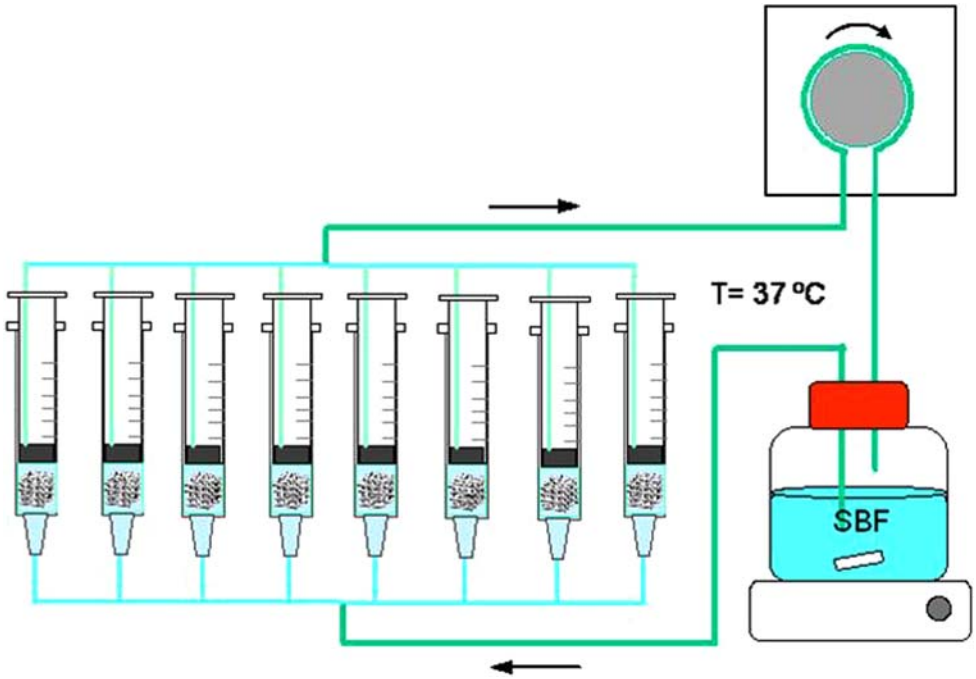

Fig. 1 Schematic drawing of the bioreactor designed for coating an apatite layer under flow perfusion

2.4 X-ray diffraction (TF-XRD)

Thin-Film X-ray Diffraction (TF-XRD, Philips X'Pert MPD, The Netherlands) was used to identify any crystalline phases present in the apatite layers formed during the immersion in SBF. The data collection was performed by 2θ scan method with 1° as incident beam angle using CuKα X-ray line and a scan speed of 0.05°/min in 2θ.

2.5 Fourier transformed infra-red (FTIR)

The chemical structure of the apatite coatings formed on the surface of the SPCL scaffold fibres after the different time periods and conditions in SBF was analysed by Fourier Transform Infrared Spectroscopy (FTIR). The surface of the fibres was scratched and the resulting particles were milled with KBr powder and shaped by compression into pellets for further analysis. All spectra were recorded using 64 scans and 2 cm^{-1} resolution in an FTIR spectrophotometer (Perkin-Elmer 1600 Series, USA).

2.6 Inductively coupled plasma spectroscopy (ICP)

The composition of the resulting Ca-P coatings was accessed by analysing the solution resulting from the dissolution of the coated scaffolds in 0.1 M HCl, under agitation for 24 h (the scaffolds were examined by SEM afterwards to confirm the total dissolution at the surface). The elemental concentration was measured by inductively coupled plasma optical emission spectroscopy (ICP-OES, JY 70 plus, Jobin Yvon, France). Duplicate samples were analysed for each condition and immersion time. From these results Ca/P ratios were calculated. The following relations were also considered: (Ca + Na + Mg + K)/P; (Ca + Mg + K)/P; Na/Ca; Mg/Ca; K/Ca in order to investigate the possible presence of Mg^{2+}, Na^{+} and K^{+} in the SBF, substituting the Ca^{2+} in the crystalline network of the apatite.

2.7 Micro-computed tomography (μ-CT)

Micro-Computed Tomography (μ-CT) of the uncoated and coated scaffolds was carried out using μ-CT 20 equipment (SCANCO Medicals, Switzerland). The X-ray scans were performed in high resolution mode of 11 μm $x/y/z$ and an integration time of 250 ms × 2 (500 ms). The rotation step used was 500/180°. The energy of the scanner used was 50 keV with 180 μA current. Around 400 slices of the materials were obtained in order to scan the entire scaffolds. Mimics from Materialise (Belgium), CT Analyser and CT Vol Realistic 3D Visualization both from SkyScan (Belgium) were used as image processing softwares, for CT reconstruction, to create and visualize the 3D representation. The 2-D histomorphometric analysis of the scaffolds was performed using a threshold of 51 to determine the porosity and a threshold of 133 to identify the apatite content along the scaffold (from 0–4500 μm) (grey values).

3 Results and discussion

3.1 Stabilization of the apatite layer

Figure 2 presents SEM micrographs of the SPCL scaffolds as processed and after the nucleation of a biomimetic apatite layer for 7 days.

3D plotting technology allowed for the processing of fibre-based 3D constructs with a controlled morphology and porosity (Fig. 2(a) and (b)) in a reproducible manner. Sodium silicate treatment followed by immersion in SBF solution for 7 days has resulted in the nucleation of a well-defined apatite layer at the surface of the fibres which covered the entire surface of these porous materials while maintaining their initial architecture (Fig. 2(c)). The mechanism for the nucleation and growth of an apatite layer on a sodium silicate gel is well known and has been described elsewhere [3, 20]. The resulting Ca-P coating presents a needle-like structure (Fig. 2(d)) corresponding to the typical morphology obtained by this biomimetic route [3]. By TF-XRD and FTIR it was possible to confirm that a poorly crystalline carbonated apatite similar to bone was formed after 7 days of immersion in SBF (data not shown). This coating was present both in the outside and in the inside of the scaffold, as it can be observed in Fig. 2(d) and (e) that present a cross-section from the interior of the scaffold, from which strong adherence of the coating to the surface of the fibres is evident. Apatite nucleation is clearly controlled by the surface [21, 22] , which serves as template for the formation of the apatite layer.

3.2 Growing of the apatite layer under static and dynamic conditions

After the formation of a stabilized bone-like apatite layer in the surface of the SPCL constructs for 7 days in static SBF, the scaffolds were divided into 3 groups and immersed in SBF solutions under 3 different hydrodynamic conditions: static, agitation and flow perfusion, for periods up to 21 days.

Figure 3 presents the typical FTIR spectra of the apatite coatings produced in the different SBF conditions, for the periods of 14 and 21 days.

The bands detected at 1630 cm^{-1} are assigned to water molecules in the apatite structure. Another broad band assigned to water was also detected in the region of 3400 cm^{-1}. In fact, apatite contains water incorporated in its structure, either chemically bonded, i.e. structural water or also adsorbed due to its hydroscopic character [23]. The bands at 866, 1412 and 1452 cm^{-1} result from the presence of carbonate (CO_3^{2-})

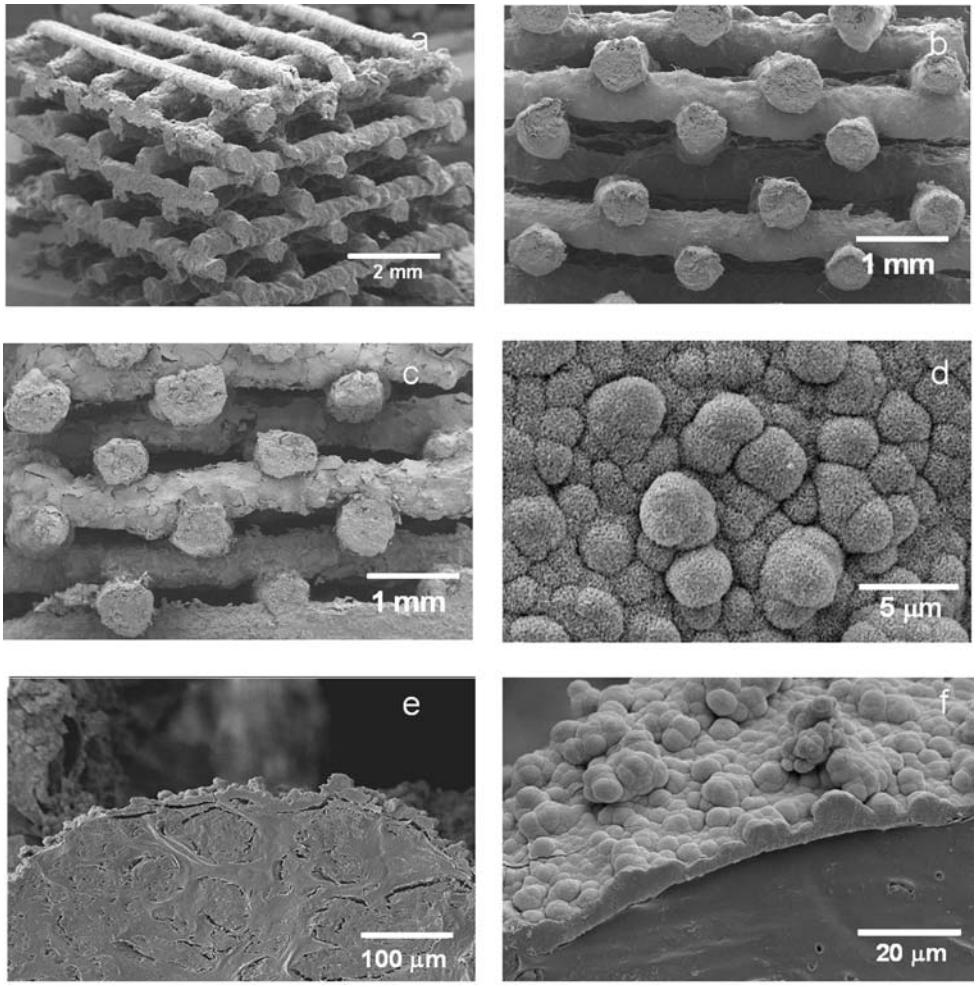

Fig. 2 SEM micrographs of SPCL scaffolds (a), (b) as processed and (c)–(f) after growing a biomimetic apatite layer for 7 days in SBF

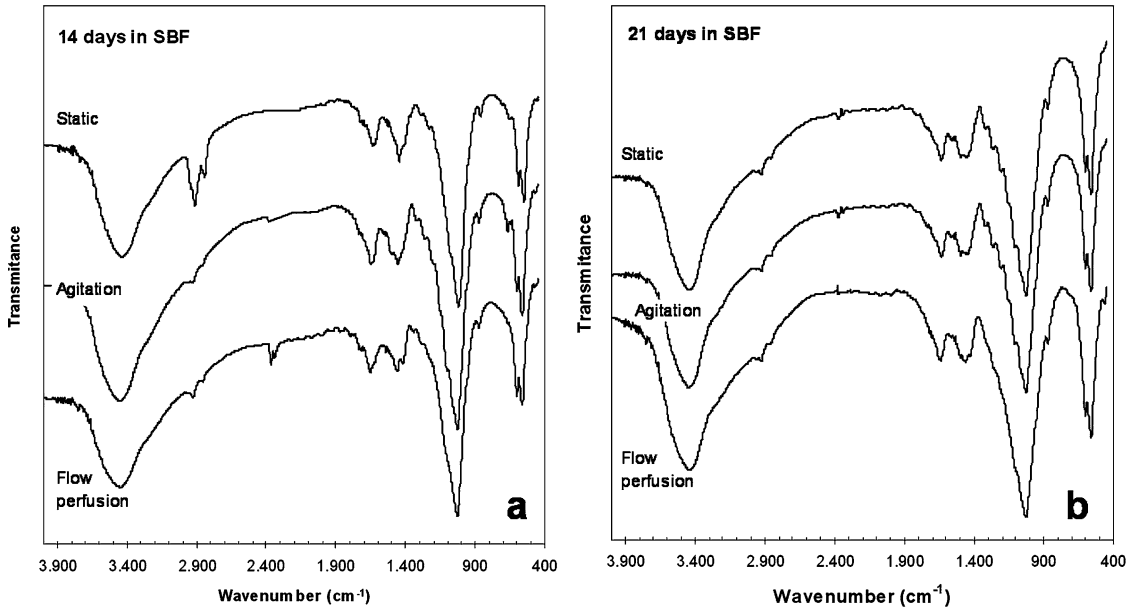

Fig. 3 FTIR spectra obtained from the analysis of apatite layers after immersion in SBF for 21 days from which 14 days under static and dynamic conditions. All the spectra were obtained from the same side of the scaffold

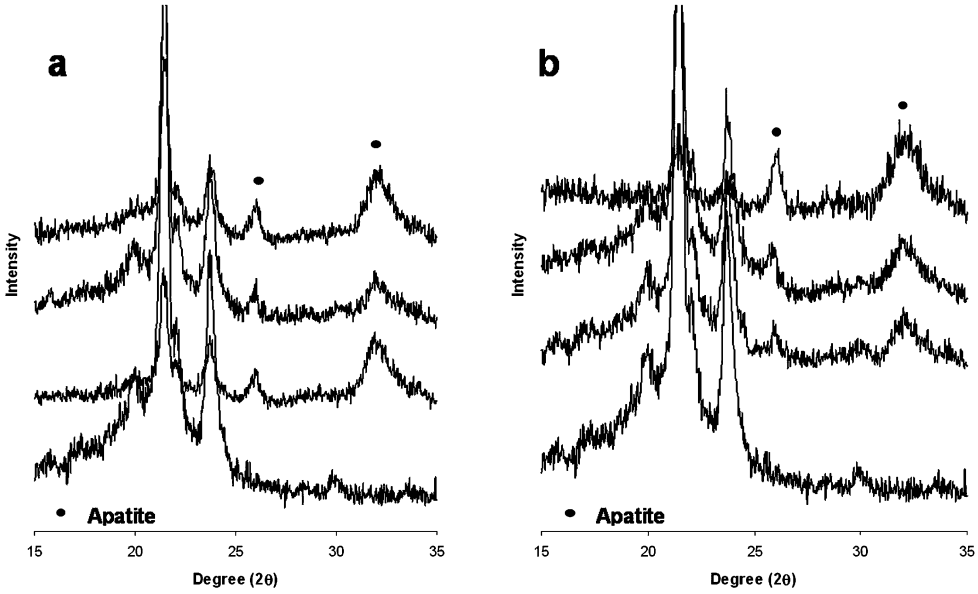

Fig. 4 TF-XRD spectra obtained from the analysis of the SPCL scaffolds before and after immersion in SBF for (a) 14 and 21 days in static and dynamic conditions

incorporated in the apatite lattice [23, 24]. The presence of these bands clearly indicates that a carbonated apatite was formed, as it is found in bone apatite. The bands at 558 and 572 are assigned to the ν_4 bending mode of the O–P–O bonds in the apatite, indicating some degree of crystallinity. The bands at 1024 cm^{-1} indicate the ν_3 stretching mode of P–O bonds [23]. The detected FTIR bands correspond to the characteristic ones of a carbonated apatite.

Figure 4 presents the typical TF-XRD spectra of the apatite coatings produced in the various static and dynamic SBF conditions.

The peaks detected at $2\theta = 20$, 21 and 24 are assigned to SPCL crystalline phases. After producing the biomimetic coatings in different conditions the main characteristic peaks attributed to HA were detected. The peak at $2\theta = 26^\circ$ is assigned to (002) plane in the apatite crystalline lattice. Another important diffraction peak is detected around $2\theta = 32^\circ$ and is related to the overlapping of planes (211, 112) and (300). This broad peak indicates that the apatite structure is composed by small crystallites. Similar XRD profiles were obtained when comparing the different static and dynamic coating conditions. From 14 to 21 days of immersion in SBF a slight increase in the intensity of the apatite peaks indicates that the apatite coatings tend to be more crystalline in the presence of SBF 1.5 ×. The intensity of the SPCL peaks diminishes considerably in case of dynamic conditions after 21 days (Fig. 3(b)), which is related with an increase of thickness of the apatite layers.

When comparing Fig. 3(a) with 3(b), and 4(a) with 4(b) no marked differences in the obtained spectra were detectable between the apatites coated after 14 days in SBF (Figs. 3(a) and 4(a)) and those coated after 21 days (Figs. 3(b) and 4(b)) or between each different condition. In the same way, FTIR and TF-XRD analysis performed to different sides in each scaffold did not reveal any clear differences in the spectra (data not shown). The presented results were obtained from the bottom side of the scaffold. By the present technique it was not possible to assess any clear modification of the chemical structure or crystallinity of the apatite layers when dynamic flows were present.

ICP analysis to the solutions resulting from dissolving the apatite coatings allowed for comparing the chemical composition of the coatings prepared under the different biomimetic conditions. In static conditions the calculated Ca/P ratio after 14 days of immersion in SBF was 1.53. Since the established value for bone-apatite is 1.67, the herein prepared biomimetic apatites are Ca-deficient. This ratio increases when considering the presence of other ions in the structure replacing for Ca such as K, Mg and Na to a value of 1.67. The elemental composition obtained for the apatite layers formed under agitation and flow perfusion is very similar (1.57 and 1.51, respectively), indicating that besides the chemical structure and crystallinity, the chemical composition of the apatite layers was also not altered by the presence of the dynamic flow conditions.

In order to evaluate the effect of the studied biomimetic procedures on the morphology and integrity of the resulting apatite layers SEM analysis was performed to the top, bottom and lateral sides of the cubic shaped scaffolds. The interior of the scaffolds was also characterized by examining cross-sections performed in the centre of the scaffolds. Therefore, these observations were intended to investigate

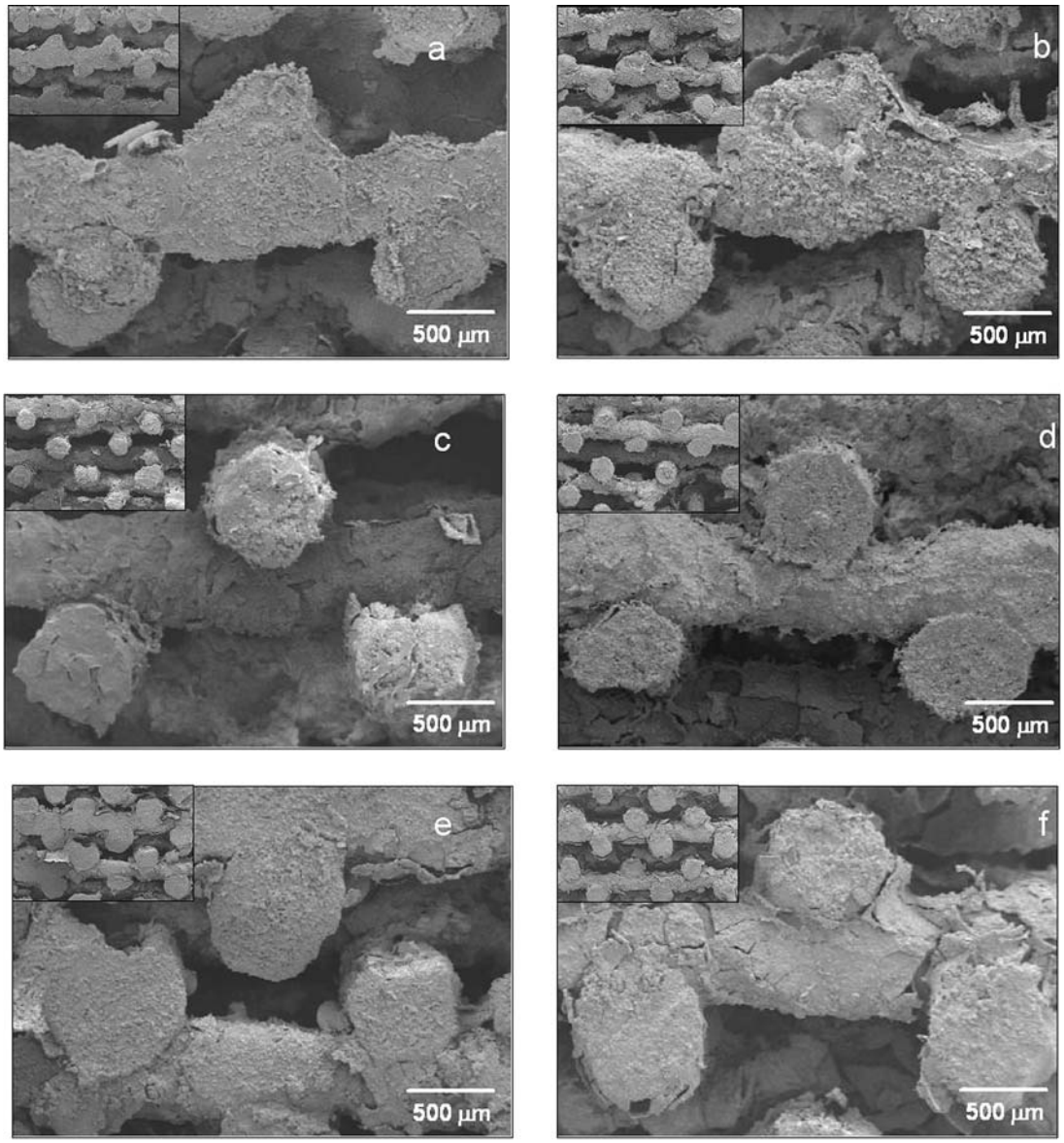

Fig. 5 SEM micrographs of the coated lateral sides of the scaffolds after immersion in SBF in static (a, b), agitation (c, d) and flow perfusion (e, f) conditions for 14 (a, c, e) and 21 (b, d, f) days

the efficiency of the methodologies on coating the overall surfaces of the constructs and were also a useful comparative mean to evaluate the applicability of the μ-CT analysis for the visualization and quantification of the apatite layers throughout the constructs.

Figure 5 presents the lateral sides of the scaffolds after being coated for 14 and 21 days in the different conditions. The correspondent cross-sections are shown in Fig. 6.

For all the studied conditions the integrity of the apatite layer nucleated in static SBF (Fig. 2(c)) was maintained during the growth stage, even when dynamic conditions were present. The apatite layers have grown and clearly covered the fibres of the scaffolds without compromising its overall morphology and porosity. Nevertheless, in case of the static condition (Figs. 5(a) and 5(b)) apatite tended to accumulate in some of the intersections of the fibres, particularly those at its outer region. A possible explanation for this effect can be a local increase of the concentration of Ca^{2+} and PO_4^{3-} ions in the SBF due to re-dissolution, in some extent, of the pre-established coating, which will induce a higher formation of apatite in those restricted areas. In case of agitation and flow perfusion conditions apatite coating has shown to better follow the fibres contour, as presented in Fig. 5(c–f). However, after 21 days some cracking of the apatite coatings was observed, particularly in case of agitation (Fig. 5(d)) and flow perfusion (Fig. 5(f)) conditions.

When considering the cross-sections of the centre of the scaffolds it is possible to confirm that for static conditions

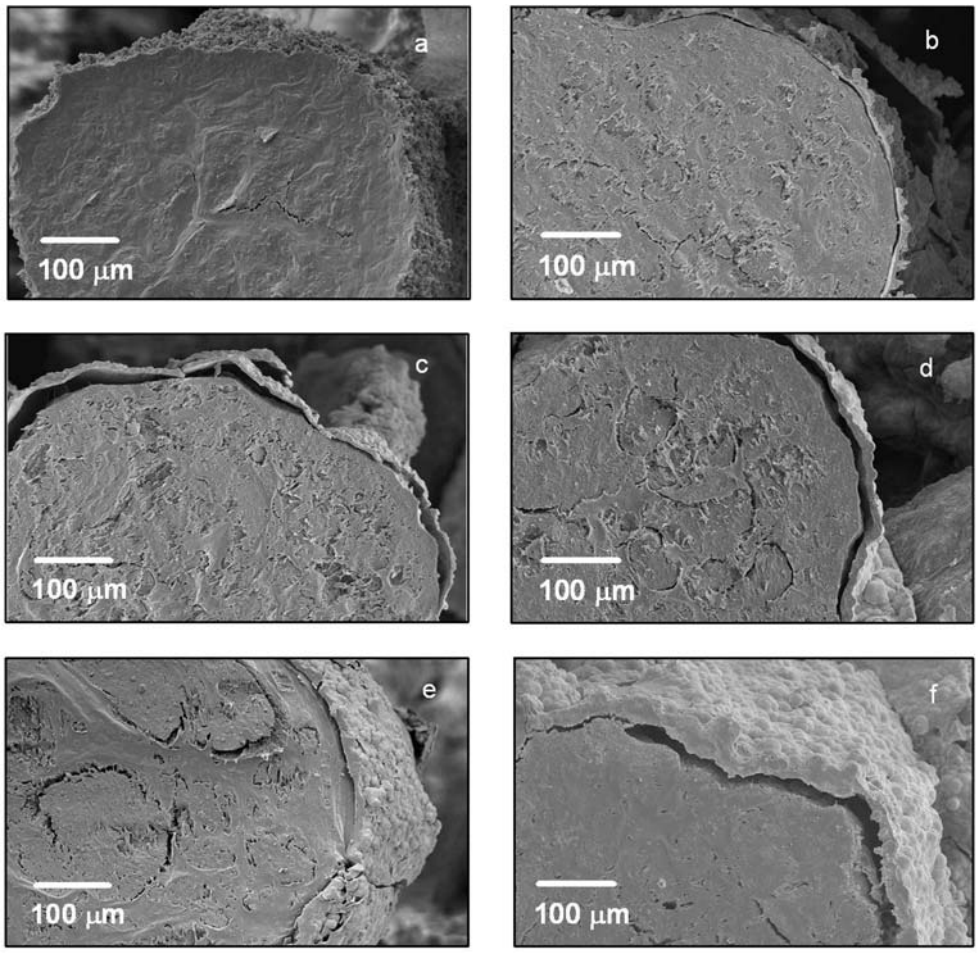

Fig. 6 SEM micrographs of the cross-sections of a fibre in the middle of the scaffold after immersion in SBF in static (a, b), agitation (c, d) and flow perfusion (e, f) conditions for 14 (a, c, e) and 21 (b, d, f) days

(Fig. 6(a) and (b)) the formed apatite layers follow the shape of the fibres while for agitation (Fig. 6(c) and (d)) a gap at the interface between the surface and the coating became visible in a considerable number of fibres. In case of flow perfusion a thicker apatite layer was formed after immersion in SBF for 14 days (Fig. 6(e) and (f)), following better the contour of the substrate. After 21 days the coating presented some extent of detachment which can be attributed mainly to the formation of a thick and cohesive apatite layer (Fig. (e)). In this case the cohesive forces tend to prevail over the adhesive forces at the interface coating/substrate. Nevertheless, one has to take into consideration that the observed coated scaffolds were previously subjected to high vacuum environments during sputtering and SEM observations and also to shear stresses during cross-section preparation which may have affected the coating integrity and adhesion. In spite of these situations, the apatite coating did not completely detach.

The calculated average thickness of the apatite layers measured *per* condition is plotted in Fig. 7. The SEM micrograph illustrates the procedure used to perform the measurements, starting from the basis of the apatite nuclei to the interface. In this way, it was assured that the measurements were performed in the same way for all the conditions. The obtained values are the minimum thickness values for all the samples.

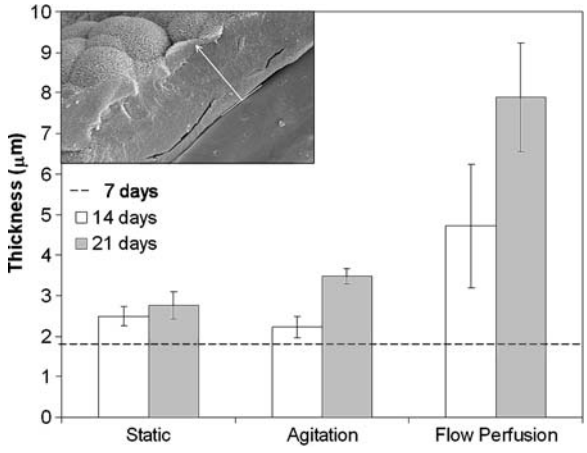

Fig. 7 Average thickness of the apatite coatings formed during the biomimetic process in static and dynamic conditions, measured by SEM analysis

The estimated apatite thickness after 7 days of immersion in SBF was $1.77 \pm 0.31\,\mu$m ($n = 6$), corresponding to a growth rate of 0.25 μm/day, during nucleation period. Subsequent immersion in SBF allowed for the apatite to grow, particularly in case of dynamic conditions. After 21 days, the calculated average thickness was $2.76 \pm 0.33\,\mu$m in static conditions, $3.47 \pm 0.19\,\mu$m in case of agitation and $7.90 \pm 1.34\,\mu$m for flow perfusion. The rates for apatite growth were respectively: 0.04, 0.17 and 0.45 μm/day. Although a continuous increase in thickness was observed, the apatite has grown at lower rates than in the nucleation stage for all the conditions since the nucleation agent (sodium silicate) was no longer participating in the mineralization process. When dynamic conditions were present the rate for apatite formation increases, which indicates that the growing process is ion transport controlled, possibly by a combination of diffusion and convection phenomena right at the interface surface/fluid [25–27].

Only a few authors have studied the induction and growth of an apatite layer on the surface of bioactive materials on dynamic SBF. In fact, to the authors' knowledge [28–32], this kind of approach has been only proposed for accessing the SBF *in vitro* mineralization of materials in with intrinsic bioactivity like silica-based ceramics [28, 30–32] or their composites [29]. However, no straight comparison can be establish with the present study due to the different and conditions used (e.g. solid/liquid ratio, flow rate) and the nature of the substrates.

3.3 μ-CT evaluation of the coated scaffolds

In the current study, μ-CT is originally used as an additional tool to complement the SEM morphological characterization, in order to evaluate the *in vitro* apatite coatings for static and dynamic conditions in 3D-plotted polymeric scaffolds as function of time. The average apatite content measured in the scaffolds is presented in Fig. 8, as function of time and static/dynamic conditions. The degree of induced *in vitro* mineralization occurring in the polymeric 3D-plotted scaffolds is presented as a percentage of the overall scaffolds' volume.

The 2D histomorphometric analysis allowed for comparing the apatite content after coating in static and dynamic conditions. After a period of 14 days, an increase in the apatite content was observed when flow perfusion was applied. The influence of dynamic conditions is even more noticeable after a coating period of 21 days for both agitation and flow perfusion conditions. As one can observe, in static conditions, the evolution of the apatite content with time is negligible. However, there is a general growth in the apatite content observed from 14 to 21 days, related with the conjugated effect of dynamic conditions and an increase in the SBF concentration (from 1 to 1.5 times). These results are consistent with

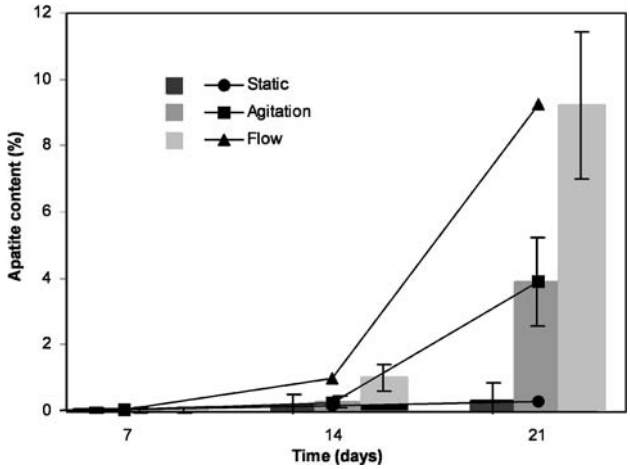

Fig. 8 *In vitro* apatite coating progress in the scaffolds measured by μ-CT as function of time and test conditions

those obtained from the examination of the cross-sections of the coated scaffolds (Fig. 6) and the correspondent thickness measurements (Fig. 7).

In Fig. 9 is plotted the SPCL porosity profile together with the apatite content distribution along the entire scaffolds as function of static and dynamic conditions for 21 days in SBF.

As expected, SPCL porosity profile obtained throughout the scaffolds presented a periodic variation, in agreement with the pre-established design of the scaffolds (Fig. 2(a)). The mean porosity of the developed scaffolds is $70.8 \pm 12\%$. As confirmed by SEM (Fig. 5) all the scaffolds were coated from the top to the bottom regardless of the coating conditions, following the porosity profile. In static conditions, the average amount of apatite detected throughout the scaffold content was below 1% (Fig. 8) of the overall polymer content. The profile of the apatite content followed the scaffolds' periodic trend although this is not clear due to the low values presented for this condition. A higher content was detected in the top of the scaffolds which can be probably related to some deposition of Ca-P precipitates in the scaffold upper side. In dynamic conditions, higher amounts of apatite were detected. In case of agitation, the periodic pattern is clearly indicating that the apatite coating follows the fibre contour. When flow perfusion is used, the coating follows in a more roughly way the periodic porosity profile but, if complemented with the SEM observations (Figs. 5 and 6), one can assure that the coating is well distributed along the fibres while following the geometry of the scaffolds. In case of flow perfusion, a general increase of the apatite coating from the top to the bottom of the 3D-plotted scaffolds is detected. In fact, for flow perfusion conditions, the side of the scaffold facing the flow will have a higher ion supply, since SBF flow rate is higher at the entrance of the chamber than in its centre. This result correlates well with the obtained values for the coating thickness presented in Fig. 7 where the calculated

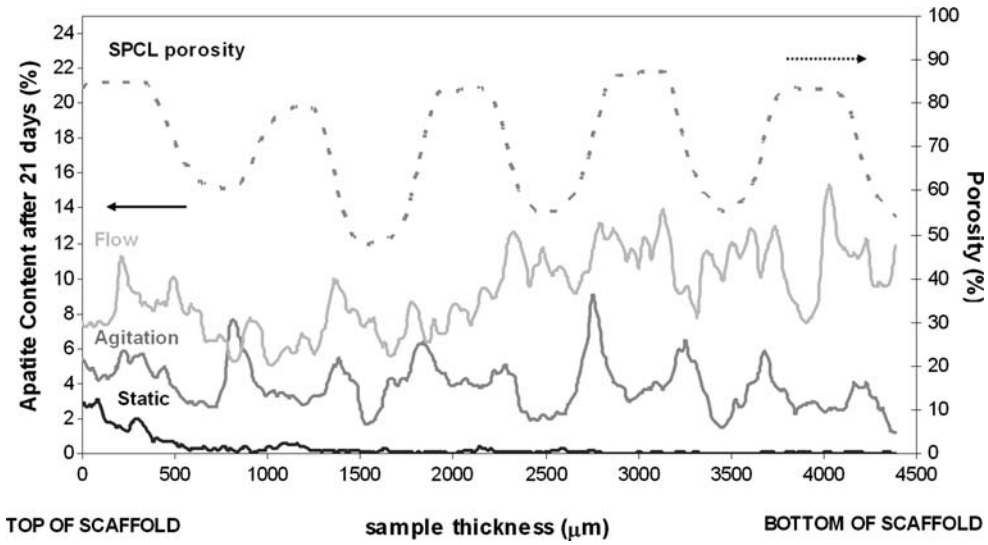

Fig. 9 SPCL porosity profile (- - -) and apatite content distribution (—) along the scaffolds after 21 days period as function of test condition

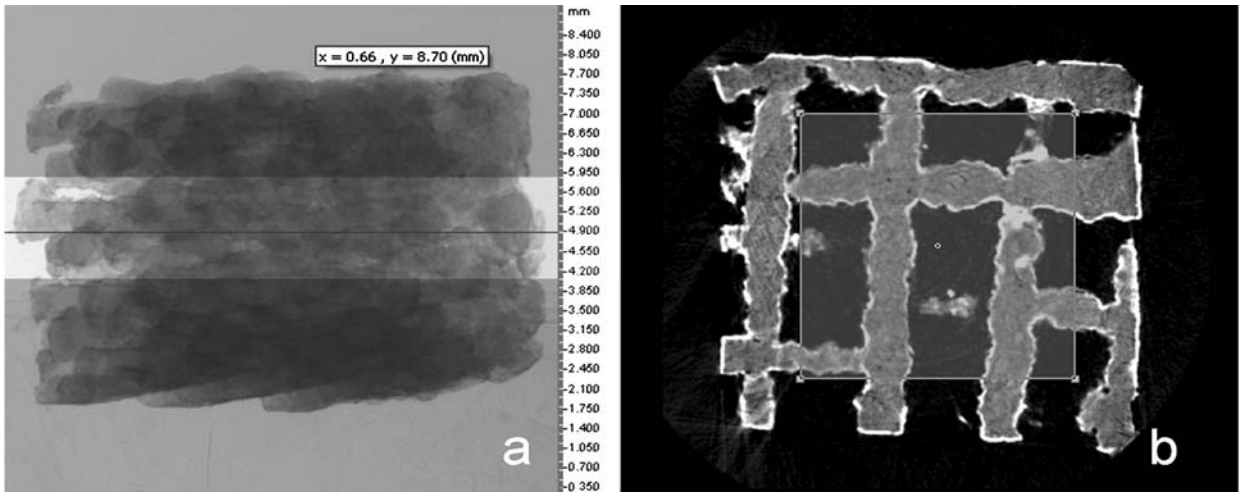

Fig. 10 Selected volume of interest (VOI) of the central and inner area of the scaffolds. This selection was applied for all the scanned scaffolds

apatite thickness presents a high standard deviation due to a thickness gradient observed from the bottom to the top of the apatite scaffolds. In fact, the fibres from the bottom surface which were facing the flow presented a higher thickness, corresponding to the values in the upper limit of the error bar. To avoid this effect, future studies will include cyclic inversion of the flow.

Although the entire scaffolds were scanned essentially for 2D histomorphometric analysis, a volume of interest (VOI) of the materials was selected from the μ-CT data set for 3D visualization. This VOI corresponds to the central and inner part of the scaffolds as illustrated in Fig. 10(a) and (b). The selection of this region included the same area used for performing the cross-sections. In this case, the main advantage of μ-CT over SEM is that sectioning is not required. Furthermore, coating of the inner part of the scaffolds is presented as a key challenge to the *in vitro* Ca-P coating technologies.

In Fig. 11 are presented different examples of cross-sections in 2D X-ray images, binary images at the pre-defined threshold used to identify the apatite content and finally, built the 3D models of the selected central VOI. The same threshold for binarization and to build the 3D models was used in all the scaffolds. These results concern a coating period of 21 days for the different tested conditions as the same trend was observed for 14 days and lower amounts of apatite.

The obtained 3D models of the apatite spatial distribution on the inner part of the scaffolds show that for static and agitation conditions the coating only partially covered the SPCL fibres. In the flow perfusion condition, a well-defined

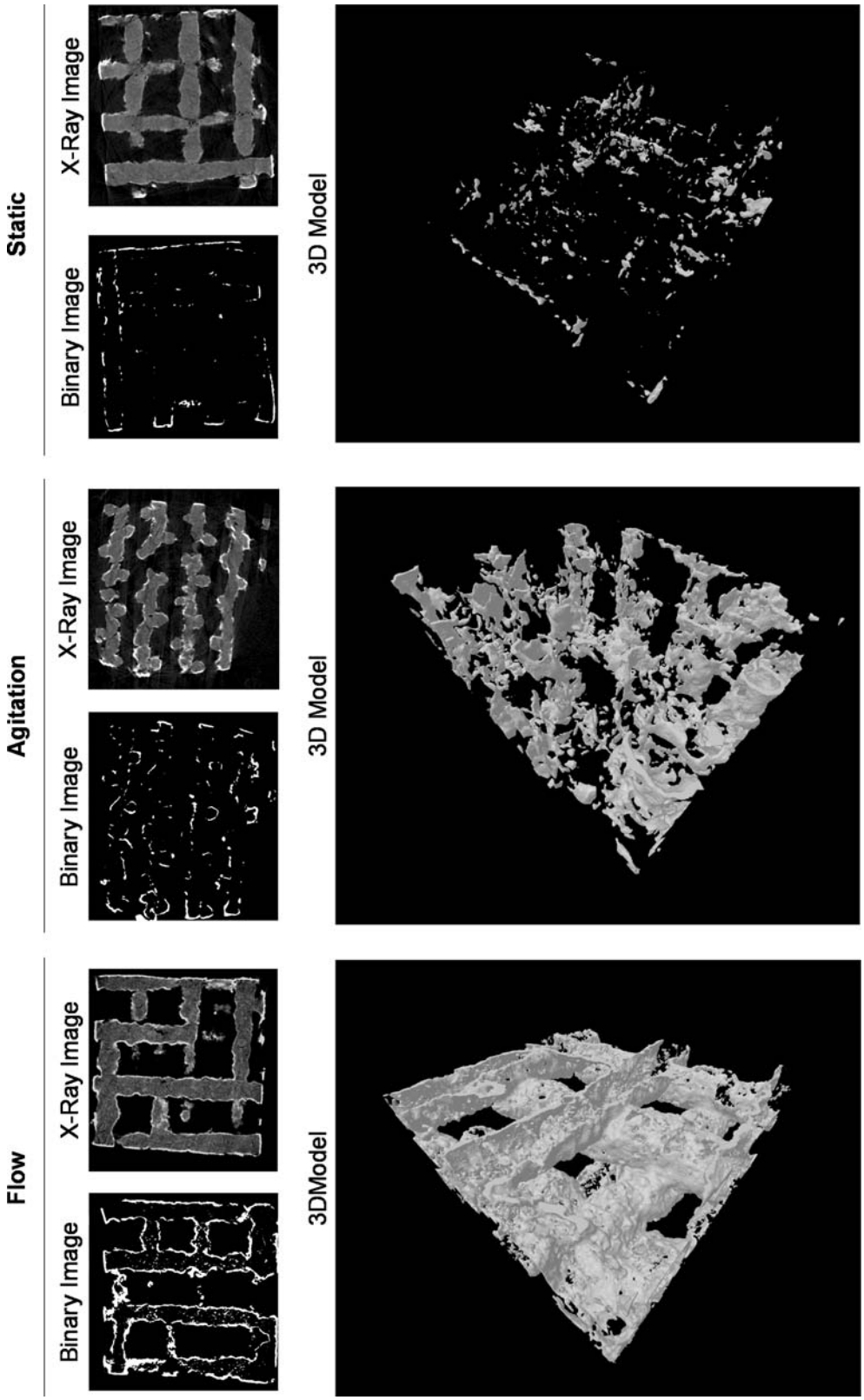

Fig. 11 2D X-ray, 2D binary images and 3D models for the apatite coatings obtained for 21 days as function of static and dynamic conditions

apatite layer covers all the inner parts of the scaffold, following the available fibre surface area without compromising the overall morphology and interconnectivity of the 3D-plotted scaffolds. By SEM examination of the different scaffolds' surfaces and cross-sections it was possible to observe the constant presence of a continuous apatite layer covering the entire fibres, which is in disagreement with the apatite 3D models for both static and agitation conditions.

This can be explained by the lower thickness of the produced apatite layers for these conditions. The resolution mode used in these scans was 11 μm, which has shown to be insufficient to detect very thin coatings. In fact, high contrasts between phases are required for better quantification [33]. Theoretically at the pre-established threshold and with the present resolution it would not be possible to visualize the correct 3D representation of apatite layers with a thickness less 11 μm (value obtained from Fig. 7). Nevertheless, one can clearly observe the coating on the scaffold in case of flow perfusion condition after 21 days in SBF, being the calculated thickness in this case around 8 μm (please see Fig. 7). As explained above, the measured thickness by SEM analysis corresponds to the minimum average values since they refer to the distance starting from the basis of the apatite nuclei to the interface of the coating. This means that considering the nuclei above the most dense layer the coating thickness will be, in average, higher that 8 μm. Furthermore, even though the resolution was 11 μm, (pixel size: 11 μm) the equipment/software is capable of detecting Ca-P coating under this limit due also to the high diffraction of this ceramic when comparing with the polymer. Of course in this case the definition is lower. In future studies high resolution should be applied (decreasing the scaffolds size and increasing, in this way, the scan magnification) in order to obtain 3D models with more reliance. The herein utilized equipment (μ-CT 20) has an optimal resolution of 8 μm/pixel. Nevertheless, by complementing with SEM observations and 2D histomorphometric analysis it is possible to state that the coating is present in all the area of the scaffolds.

Microtomograph histomorphometric analysis revealed to be a useful complementary tool to characterize the induced *in vitro* mineralization and study different static and dynamic influence in the coatings growing. The apatite coating can be also quantified in terms of the overall scaffolds volume and its distribution along the scaffolds can be easily assessed without damaging the constructs. Nevertheless, the correct choice of adequate thresholds and the use of high resolution modes are extremely important steps in order to obtain the correct visualization of the apatite coatings. The herein presented results provide the first insights on the potential of this non-destructive technique for the overall morphological characterization of biomimetic apatite layers, which would be impossible to achieve with the currently used techniques.

μ-CT analysis has clearly demonstrated that flow perfusion was the most effective apatite coating procedure, as already indicated by SEM technique. The advantages of this system when comparing with simple agitation and static conditions are numerous: (i) unlike static conditions, the accumulation of precipitates is avoided; (ii) it can closer mimic in vivo apatite mineralization; (iii) a higher control of coating process is achieved by the controlling the flow rate; (iv). the scaffolds and the coatings can better preserve their integrity because they are static in the chamber, which does not occur for agitation condition; (v) a higher rate for apatite formation is obtained which means that the time for the coating process can be greatly reduced. Moreover, flow perfusion conditions can allow for the sequential incorporation of biologically interesting molecules in the context of TE. This subject together with studies on cell differentiation and proliferation will be investigated in the future.

4 Conclusions

Static and dynamic biomimetic routes allow for the effective coating of a bone-like apatite layer on newly developed SPCL scaffolds. Dynamic conditions mimic better the biological milieu, allowing for the coating of complex architectures at higher rates for the production the apatite layers, particularly in case of flow perfusion. By this process the time required for apatite formation was highly reduced and more stable and well-defined apatite layers were formed. Morphological analysis by SEM and μ-CT gave valuable information on the architecture of the scaffolds and on the dimension and distribution of the coatings. The herein presented results, obtained using μ-CT, provided the first insights on the potential of this non-destructive technique for the overall morphological characterization of biomimetic apatite layers, which would be impossible to achieve with the typically used characterization techniques.

Acknowledgments Portuguese Foundation for Science and Technology (Ph.D. grant to A. L. Oliveira, SFRH/BD/10956/2002 and Pos-Doc grant to Rui Amandi de Sousa, SFRH/BPD/17151/2004, under the POCTI Program). This work was partially supported by FCT through POCTI and/or FEDER programmes and also partially supported by the EU Project HIPPOCRATES (NMP3-CT-2003-505758) and EXPERTISSUES (NMP-CT-2004-500283). Materialise (Belgium) for MIMICS® software and Gerald Zanoni from Ludwig Boltzmann Institute for Experimental and Clinical Traumatology (Austria) for the μ-CT scans in the scope of the referred EU projects.

References

1. A. L. OLIVEIRA, J. F. MANO and R. L. REIS, *Curr. Opin. Solid. St. M* **7** (2003) 309.
2. Y. ABE, T. KOKUBO and T. YAMAMURO, *J. Mater. Sci.-Mater. M.* **1** (1990) 233.

3. A. L. OLIVEIRA, P. B. MALAFAYA and R. L. REIS, *Biomaterials* **24** (2003) 2575.
4. A. L. OLIVEIRA and R. L. REIS, *J. Mater. Sci.: Mater. Med.* **15** (2004) 533.
5. L. MULDER, J. H. KOOLSTRA and T. M. G. J. VAN EUDEN, *Acta. Radiol.* **45** (2004) 769.
6. R. A. KUBIK-HUCH, W. DORFFLER, G. K. VON SCHULTHESS, B. MARINCEK, O. R. KOCHLI, B. SEIFERT, U. HALLER and H. C. STEINERT, *Eur. Radiol.* **10** (2000) 761.
7. P. THURNER, B. MULLER, U. SENNHAUSER, J. HUBBELL and R. MULLER, *J. Phys.-Condens Mat.* **16** (2004) S3499.
8. M. ITO, *J. Bone. Miner. Metab.* **23** (2005) 115.
9. S. CARTMELL, K. HUYNH, A. LIN, S. NAGARAJA and R. GULDBERG, *J. Biomed. Mater. Res. A.* **69A** (2004) 97.
10. V. J. CHEN, L. A. SMITH and P. X. MA, *Biomaterials* **27** (2006) 3973.
11. R. L. REIS and A. M. CUNHA, *J. Mater. Sci.: Mater. Med.* **6** (1995) 786.
12. C. ELVIRA, J. F. MANO, J. SAN ROMAN and R. L. REIS, *Biomaterials* **23** (2002) 1955.
13. M. E. GOMES and R. L. REIS, *Int. Mater. Rev.* **49** (2004) 261.
14. P. B. MALAFAYA, C. ELVIRA, A. GALLARDO, J. SAN ROMAN and R. L. REIS, *J. Biomater. Sci. Polym. Ed.* **12** (2001) 1227.
15. S. V. I. GOMES, M. E. BEHRAVESH, E. REIS, R.L. MIKOS and G. ANTONIOS, *J. Biomed. Mater. Res.* **67A** (2003) 87.
16. K. TUZLAKOGLU, N. BOLGEN, A. J. SALGADO, M. E. GOMES, E. PISKIN and R. L. REIS, *J. Mater. Sci. Mater. Med.* **16** (2005) 1099.
17. M. E. GOMES, R. L. REIS, A. M. CUNHA, C. A. BLITTERSWIJK and J. D. DE BRUIJN, *Biomaterials* **22** (2001) 1911.
18. D. W. HUTMACHER, M. SITTINGER and M. V. RISBUD, *Trends. Biotechnol.* **22** (2004) 354.
19. T. KOKUBO, H. KUSHITANI, S. SAKKA, T. KITSUGI and T. YAMAMURO, *J. Biomed. Mater. Res.* **24** (1990) 721.
20. H. TAKADAMA, H. M. KIM, T. KOKUBO and T. NAKAMURA, *Chem. Mater.* **13** (2001) 1108.
21. W. J. WU, D. E. GERARD and G. H. NANCOLLAS, *J. Am. Soc. Nephrol.* **10** (1999) S355.
22. W. J. WU and G. H. NANCOLLAS, *Phosph. Sulfur and Silicon Rel. Elem.* **146** (1999) 125.
23. M. VALLET-REGI, A. M. ROMERO, C. V. RAGEL and R. Z. LEGEROS, *J. Biomed. Mater. Res.* **44** (1999) 416.
24. I. REHMAN and W. BONFIELD, *J. Mater. Sci-Mater. M.* **8** (1997) 1.
25. W. J. WU and G. H. NANCOLLAS, *Adv, Colloid Interf. Sci.* **79** (1999) 229.
26. K. HATA, T. KOKUBO, T. NAKAMURA and T. YAMAMURO, *J. Am. Ceram. Soc.* **78** (1995) 1049.
27. T. KOKUBO, H. M. KIM, M. KAWASHITA, H. TAKADAMA, T. MIYAZAKI, M. UCHIDA and T. NAKAMURA, *Glass. Sci. Technol.* **73** (2000) 247.
28. A. RAMILA and M. VALLET-REGI, *Biomaterials* **22** (2001) 2301.
29. D. EGLIN, S. A. M. ALI and C. C. PERRY, *J. Biomed. Mater. Res. A.* **69A** (2004) 718.
30. M. VALLET-REGI, J. PEREZ-PARIENTE, I. IZQUIERDO-BARBA and A. J. SALINAS, *Chem. Mater.* **12** (2000) 3770.
31. P. SIRIPHANNON, Y. KAMESHIMA, A. YASUMORI, K. OKADA and S. HAYASHI, *J. Biomed. Mater. Res.* **60** (2002) 175.
32. A. J. SALINAS, M. VALLET-REGI and I. IZQUIERDO-BARBA, *J. Sol-Gel. Sci. Techn.* **21** (2001) 13.
33. W. SUN and P. LAL, *Comput. Meth. Prog. Bio.* **67** (2002) 85.